

Antiferromagnetic critical point on graphene's honeycomb lattice: A functional renormalization group approach

Lukas Janssen^{1,2,*} and Igor F. Herbut^{1,3}

¹*Department of Physics, Simon Fraser University, Burnaby, British Columbia, Canada V5A 1S6*

²*Theoretisch-Physikalisches Institut, Friedrich-Schiller-Universität Jena, Max-Wien-Platz 1, 07743 Jena, Germany*

³*Max-Planck-Institut für Physik komplexer Systeme, Nöthnitzer Str. 38, 01187 Dresden, Germany*

Electrons on the half-filled honeycomb lattice are expected to undergo a direct continuous transition from the semimetallic into the antiferromagnetic insulating phase with increase of on-site Hubbard repulsion. We attempt to further quantify the critical behavior at this quantum phase transition by means of functional renormalization group (RG), within an effective Gross-Neveu-Yukawa theory for an $SO(3)$ order parameter (“chiral Heisenberg universality class”). Our calculation yields an estimate of the critical exponents $\nu \simeq 1.31$, $\eta_\phi \simeq 1.01$, and $\eta_\psi \simeq 0.08$, in reasonable agreement with the second-order expansion around the upper critical dimension. To test the validity of the present method we use the conventional Gross-Neveu-Yukawa theory with \mathbb{Z}_2 order parameter (“chiral Ising universality class”) as a benchmark system. We explicitly show that our functional RG approximation in the sharp-cutoff scheme becomes one-loop exact both near the upper as well as the lower critical dimension. Directly in $2 + 1$ dimensions, our chiral-Ising results agree with the best available predictions from other methods within the single-digit percent range for ν and η_ϕ and the double-digit percent range for η_ψ . While one would expect a similar performance of our approximation in the chiral Heisenberg universality class, discrepancies with the results of other calculations here are more significant. Discussion and summary of various approaches is presented.

I. INTRODUCTION

Graphene is an excellent conductor. Experiments show that this remains true even for suspended graphene sheets, when the substrate is removed.¹ Recent accurate *ab initio* computations of the strength of Coulomb repulsion in free-standing graphene, however, find values which would place graphene not too far from the quantum phase transition into a putative Mott-insulating phase.^{2,3} It is thus not inconceivable that there exist situations in which the Coulomb interaction between the electrons would become strong enough relative to the bandwidth, so that a band gap in the electronic spectrum is dynamically generated. Such an effect may, for example, be observed in mechanically stretched graphene sheets, where the hopping of the electrons between neighboring sites would (albeit most likely non-uniformly) be reduced. Tuning through a semimetal–Mott-insulator phase transition could facilitate extraordinary applications for graphene-based electronics, and would therefore be also highly desirable from a technological point of view. On the other hand, because of its Dirac-type spectrum, a Mott transition in graphene mimics the spontaneous symmetry breakdown in high-energy particle physics, as it occurs in the strong and electroweak sectors. Understanding the correlated physics of graphene near criticality can therefore, as it has already, fertilize further the research on some of the most intriguing issues of modern fundamental physics: chiral symmetry breaking in QCD, the electroweak phase transition and the Higgs mechanism, and the triviality problem in asymptotically nonfree sectors of the standard model of particle physics.

The nature of the quantum phase transition on graphene's honeycomb lattice has been under much

debate.^{4–6} Recently, however, the results began to converge towards the scenario with a single second-order phase transition between the semimetallic and Mott-insulating states: Analytical results for all perturbatively accessible deformations of the theory near $1 + 1$ ⁷ and $3 + 1$ ⁸ dimensions, and in the $1/N$ ^{5,9} expansion, suggest that the strength of the long-range part ($\sim 1/r$) of the Coulomb interaction, at least when not too strong and at accessible length scales, is a marginally irrelevant coupling, and that the transition is triggered by strong short-range components of the interaction.⁷ For the Hubbard model on the honeycomb lattice, recent quantum Monte Carlo (MC) calculations find for strong on-site repulsion a direct and continuous quantum phase transition into the antiferromagnetic insulator.^{10,11} Universality suggests that the transition should be within the $SU(2)$ -Gross-Neveu (“chiral Heisenberg”) universality class and the scaling behavior of the MC data indeed fits persuasively well to the predictions from the first-order ϵ -expansion of the $SU(2)$ -Gross-Neveu-Yukawa field theory.¹¹ A reliable calculation of the critical exponents is, as always, a challenging task and—very similar to the much investigated bosonic $O(N)$ universality classes—accurate numerical estimates for the universal quantities in $2 + 1$ dimensions can only be obtained by convergence of results from several complementary approaches.¹² However, besides the ϵ -expansion results^{8,13} and the quantum Monte Carlo on honeycomb lattice,^{10,11} there are to date no other predictions for the critical exponents of the chiral Heisenberg universality class available.

The aim of this article is therefore to attempt to further quantify the critical behavior of the chiral Heisenberg universality class by means of functional renormalization group (RG) methods. The functional RG has success-

fully been used to describe a variety of different correlated fermion systems.^{14,15} In the context of graphene it has been employed to determine the dominant instabilities on single-layer,¹⁶ bilayer,¹⁷ and trilayer¹⁸ honeycomb lattices at and away¹⁹ from half filling. By taking collective (Hubbard-Stratonovich-type) degrees of freedom into account, the functional RG has been shown to be an excellent tool to describe $(2+1)$ -dimensional relativistic fermion models at criticality.^{20–27}

We first use the \mathbb{Z}_2 -Gross-Neveu (“chiral Ising”) universality class as a benchmark system to estimate the validity of our approximation. The chiral Ising universality class is supposed to describe the transition into a “charge density wave” (CDW) phase, with a broken sublattice symmetry, favored by a large nearest-neighbor repulsion on the honeycomb lattice.^{5,16} Critical exponents have been computed to 3rd loop order near $D = 1 + 1$ space-time dimensions (with the anomalous dimensions up to 4th order),^{28–32} to 2nd order near $D = 3 + 1$ dimensions,^{13,33} to 2nd order in the $1/N_f$ -expansion (with the fermionic anomalous dimension up to 3rd order),^{34,35} using Monte-Carlo simulations,³³ as well as functional RG methods.^{20–22}

The loop corrections in the expansions are generically only slowly (or even not at all) decreasing with the order, such that the naive extrapolation to the physical case with $\epsilon = 1$ and/or $N_f = 2$ is often not without problems. Due to the lack of knowledge of the large-order behavior of the coefficients, standard Borel-type resummation techniques appear to be hardly justified. We argue that a sensible resummation of the ϵ -expansions can be obtained by using the information from the $(2 + \epsilon)$ -expansion and the $(4 - \epsilon)$ -expansion *simultaneously* in terms of an interpolation between those two limits. For the chiral Ising universality class, we show that our functional RG results in the sharp-cutoff scheme become one-loop exact both near the upper as well as the lower critical dimension, and that for a general dimension $2 < D < 4$ they agree remarkably well with the proposed interpolational resummations. They also agree with the predictions from all other methods within the mid single-digit percent range for ν and η_ϕ and the lower double-digit percent range for η_Ψ ; see Table I.

For the chiral Heisenberg universality class, which is assumed to describe the antiferromagnetic phase transition on the honeycomb lattice, much fewer results are available at the moment. Within the functional RG approach we obtain estimates for the critical behavior in terms of the correlation length exponent ν , the anomalous dimensions for order parameter η_ϕ and for the fermionic field η_Ψ , as well as the corrections-to-scaling exponent ω ; see Table II. Our results for ν and η_ϕ agree reasonably well with the previous second-order ϵ -expansion, whereas the result for η_Ψ is significantly different. The results in $D = 2+1$ are also numerically quite different from the lowest-order ϵ -expansion,⁸ which on the other hand, agrees surprisingly well with the Monte Carlo study of the Hubbard model on honeycomb lattice.¹¹ More nu-

merical and analytical studies of this universality class are obviously needed.

The rest of the article is organized as follows: In the next section we describe our effective model, its symmetries and breaking patterns. A brief introduction to the functional RG approach is given in Sec. III, and the flow equations are derived in Sec. IV. In Sec. V we discuss the fixed points first by expanding around the upper critical dimension, thereby confirming previous Wilsonian RG ϵ -expansion results, and eventually by numerically evaluating the full set of flow equations for general space-time dimension $2 < D < 4$. We discuss our results and compare them extensively with the existing literature in Sec. VI. Conclusions are presented in Sec. VII.

II. EFFECTIVE THEORY

The spin-1/2 electrons on the honeycomb lattice are described by the 8-component Dirac fermion fields $\Psi = \begin{pmatrix} \Psi_\uparrow \\ \Psi_\downarrow \end{pmatrix}$ and its Dirac conjugate $\bar{\Psi} = \Psi^\dagger(\mathbb{1}_2 \otimes \gamma_0)$ in $2 < D < 4$ space-time dimensions. $\Psi_{\uparrow,\downarrow}$ denote the two four-component spinors for direction up and down of the physical spin. Due to the increase of the Fermi velocity v_F near half filling,¹ the weak long-range part of the static Coulomb interaction (effective graphene fine-structure constant) appears to be an irrelevant coupling, and near the criticality Lorentz invariance is emergent.^{5,7–9} The divergence of v_F , of course, is an artifact of the static model, and the Fermi velocity ultimately can not exceed the velocity of light. The critical exponents we compute in the following will thus in principle receive corrections of the order of the QED fine-structure constant $\simeq 1/137$.³⁶ In any realistic experimental or numerical setup the running of v_F is bound by finite temperature and the system’s size. In our model we will henceforth ignore these corrections, and retain only the short-range parts of the Coulomb repulsion.⁷ The Euclidean effective theory describing the Mott transition with integrated-out Coulomb field is then explicitly relativistic; it is given in terms of Ψ , $\bar{\Psi}$, and the order parameter field ϕ_a as⁸

$$\mathcal{S} = \int d\tau d^{D-1}\vec{x} \left[\bar{\Psi}(\mathbb{1}_2 \otimes \gamma_\mu) \partial_\mu \Psi + \frac{1}{2} \phi_a (\bar{m}^2 - \partial_\mu^2) \phi_a + \bar{\lambda} (\phi_a^2)^2 + \bar{g} \phi_a \bar{\Psi}(\sigma_a \otimes \mathbb{1}_4) \Psi \right], \quad (1)$$

with the space-time index $\mu = 0, 1, \dots, D - 1$, the D -derivative $(\partial_\mu) = (\partial_\tau, \vec{\nabla})$ and the 4×4 gamma matrices, obeying the Clifford algebra $\{\gamma_\mu, \gamma_\nu\} = 2\delta_{\mu\nu}$. Summation over repeated indices is assumed. The overbar emphasizes the dimensionfulness of the coupling constants $\bar{\lambda}$ and \bar{g} . In the direct products $\sigma_a \otimes \gamma_\mu$ the Pauli matrices act on spin, and the gamma matrices act on Dirac indices. The index a either runs from 1 to 3, to which we will refer to as “chiral Heisenberg”¹³ model in the follow-

ing, or it is fixed $a \equiv 0$ with $\sigma_0 \equiv \mathbb{1}_2$. We will refer to the latter case as “chiral Ising”¹³ model. The standard Ising and Heisenberg universality classes can be recovered from the chiral models by artificially setting $\bar{g} \equiv 0$. Our chiral systems thus agree with their purely bosonic (non-chiral) counterparts in terms of the order-parameter symmetry. They differ, however, in that they incorporate massless (chiral) fermionic modes, and they thus describe different universality classes. In 2 + 1 dimensions we may use the “graphene” representation⁵ $\gamma_0 = \mathbb{1}_2 \otimes \sigma_z$, $\gamma_1 = \sigma_z \otimes \sigma_y$, and $\gamma_2 = \mathbb{1}_2 \otimes \sigma_x$. In this representation the Grassmann fields u and v on the two sublattices of the honeycomb lattice near the Dirac point \vec{K} are related to the Dirac field as

$$\Psi_\sigma^\dagger(\vec{x}, \tau) = \int \frac{d\omega d^{D-1}\vec{q}}{(2\pi)^D} e^{i\omega\tau + i\vec{q}\cdot\vec{x}} \left[u_\sigma^\dagger(\vec{K} + \vec{q}, \omega), v_\sigma^\dagger(\vec{K} + \vec{q}, \omega), u_\sigma^\dagger(-\vec{K} + \vec{q}, \omega), v_\sigma^\dagger(-\vec{K} + \vec{q}, \omega) \right], \quad (2)$$

where we have chosen a reference frame in which $q_x = \vec{q} \cdot \vec{K}/|K|$, and for simplicity have set the lattice spacing and the Fermi velocity to unity. There are two further 4×4 matrices which anticommute with all three γ_μ : $\gamma_3 = \sigma_x \otimes \sigma_y$ and $\gamma_5 = \sigma_y \otimes \sigma_y$. The Hermitian product $\gamma_{35} = -i\gamma_3\gamma_5$ commutes with the γ_μ 's and anticommutes with γ_3 and γ_5 . Note that it is diagonal in our representation.

Let us discuss the symmetries of our effective relativistic models and relate them to the structure of the underlying honeycomb lattice. The action in Eq. (1) exhibits a discrete reflection symmetry,

$$\mathbb{Z}_2 : \Psi \mapsto (\mathbb{1}_2 \otimes \gamma_2)\Psi, \quad \bar{\Psi} \mapsto -\bar{\Psi}(\mathbb{1}_2 \otimes \gamma_2), \quad \phi_a \mapsto -\phi_a, \quad (3)$$

with the (spatial) momentum reflected across the first axis: $q_x \mapsto q_x$, $q_y \mapsto -q_y$. Again, $a \equiv 0$ in the chiral Ising model and $a = 1, 2, 3$ in the chiral Heisenberg model, respectively. This defines the sublattice-exchange symmetry of the honeycomb lattice, which exchanges the two Grassmann fields $u \leftrightarrow v$.³⁷ Both models are furthermore invariant under $SU(2)$ spin rotations, under which ϕ_0 is a scalar and $\vec{\phi} = (\phi_a)_{a=1,2,3}$ transforms as a vector:

$$SU(2)_{\text{sp}} : \Psi \mapsto e^{i\theta\vec{n}\cdot(\vec{\sigma}\otimes\mathbb{1}_4)}\Psi, \quad \bar{\Psi} \mapsto \bar{\Psi}e^{-i\theta\vec{n}\cdot(\vec{\sigma}\otimes\mathbb{1}_4)}, \\ \phi_0 \mapsto \phi_0, \quad \vec{\phi} \mapsto R\vec{\phi}, \quad (4)$$

with rotation matrix $(R_{ab}) = (\delta_{ab} - 2\theta\epsilon_{abc}n_c) \in O(3)$. Here, we have used $[(\sigma_a \otimes \mathbb{1}_4), (\sigma_b \otimes \mathbb{1}_4)] = 2\epsilon_{abc}(\sigma_c \otimes \mathbb{1}_4)$, ensuring that the chiral Heisenberg bilinear $\bar{\Psi}(\vec{\sigma} \otimes \mathbb{1}_4)\Psi$ transforms as a vector under $SU(2)_{\text{sp}}$. Charge conservation requires the usual $U(1)_{\text{ch}}$ phase-rotational symmetry $\Psi \mapsto e^{i\theta}\Psi$, $\bar{\Psi} \mapsto \bar{\Psi}e^{-i\theta}$. However, the charge in each Dirac-cone sector at wavevectors $\pm\vec{K}$ is conserved separately, and the phases of the modes in the two valleys can therefore be rotated independently. Formally, this can be seen by making use of the “chiral” projector

$P_\pm = \mathbb{1}_2 \otimes (\mathbb{1}_4 \pm \gamma_{35})/2$, which projects onto the modes near $\pm\vec{K}$. The corresponding “chiral” $U(1)$ symmetry is

$$U(1)_\chi : \Psi \mapsto e^{i\theta(\mathbb{1}_2 \otimes \gamma_{35})}\Psi, \quad \bar{\Psi} \mapsto \bar{\Psi}e^{-i\theta(\mathbb{1}_2 \otimes \gamma_{35})}. \quad (5)$$

On the honeycomb lattice, $U(1)_\chi$ in fact corresponds to translational invariance.³⁷ Additional to the phase rotations, in the chiral Ising model the two modes at $\pm\vec{K}$ can also be rotated independently in spin space. The chiral symmetry here is thus elevated to $U(2)_\chi \simeq U(1)_\chi \times SU(2)_\chi$, with

$$SU(2)_\chi : \Psi \mapsto e^{i\theta\vec{n}\cdot(\vec{\sigma}\otimes\gamma_{35})}\Psi, \quad \bar{\Psi} \mapsto \bar{\Psi}e^{-i\theta\vec{n}\cdot(\vec{\sigma}\otimes\gamma_{35})}, \quad (6)$$

while keeping the order-parameter field $\phi_0 \mapsto \phi_0$ fixed. In the chiral Heisenberg model, however, since the commutator $[(\sigma_a \otimes \gamma_{45}), (\sigma_b \otimes \mathbb{1}_4)]$ is *not* proportional to $\sigma_c \otimes \mathbb{1}_4$, the bilinear $\bar{\Psi}(\vec{\sigma} \otimes \mathbb{1}_4)\Psi$ is not a vector under $SU(2)_\chi$. Hence, the chiral symmetry here is not elevated, and remains $U(1)_\chi$. Altogether, the symmetry groups of the chiral Ising and the chiral Heisenberg model therefore are

$$\chi\text{-Ising} : \mathbb{Z}_2 \times SU(2)_{\text{sp}} \times U(1)_{\text{ch}} \times U(2)_\chi, \quad (7)$$

$$\chi\text{-Heisenberg} : \mathbb{Z}_2 \times SU(2)_{\text{sp}} \times U(1)_{\text{ch}} \times U(1)_\chi. \quad (8)$$

For strong coupling the order-parameter field can develop a nonvanishing vacuum expectation value (VEV). In the chiral Ising case with a single order-parameter field ($a \equiv 0$) a VEV $\langle\phi_0\rangle \propto \langle\bar{\Psi}\Psi\rangle \neq 0$ breaks the \mathbb{Z}_2 sublattice-exchange symmetry spontaneously, and our model describes the second-order transition into the staggered-density phase, the charge density wave (CDW) state. The critical behavior is described by the celebrated \mathbb{Z}_2 -Gross-Neveu (= chiral Ising) universality class, the corresponding universal exponents being fairly well known.^{8,13,20–23,28–35} In contrast, the chiral Heisenberg model with the 3-vector order-parameter field $\vec{\phi} = (\phi_1, \phi_2, \phi_3)$ describes the transition of the semimetallic phase into the staggered-magnetization state, the antiferromagnetic (AFM) phase. If $\vec{\phi}$ develops a VEV, $\langle\vec{\phi}\rangle \propto \langle\bar{\Psi}(\vec{\sigma} \otimes \mathbb{1}_4)\Psi\rangle \neq \vec{0}$, both the \mathbb{Z}_2 sublattice-exchange symmetry as well as the $SU(2)_{\text{sp}}$ spin-rotational symmetry are spontaneously broken down to a residual $O(2) \simeq U(1)$ symmetry. On the AFM side of the transition we therefore expect 2 massless bosonic modes, the Goldstone modes, corresponding to the field variables being orthogonal to the VEV. The corresponding chiral Heisenberg [= $SU(2)$ -Gross-Neveu] universality class is not so well understood (see, however, Refs. 8,13 for results within an expansion around the upper critical dimension). In the following, we will investigate both the chiral Ising and the chiral Heisenberg universality classes by means of the functional renormalization group.

III. FUNCTIONAL RENORMALIZATION GROUP

The functional renormalization group (FRG) approach is an efficient tool to compute the generating functional of the one-particle irreducible correlation functions—the effective action $\Gamma[\phi_a, \Psi, \bar{\Psi}]$ ⁵³. For reviews on this rapidly evolving method, applied to both condensed-matter as well as high-energy physics, see Refs. 14,15,23,38–45. A thorough and very pedagogical introduction can be found in Ref. 46. The central object of the method is the scale-dependent *effective average action* $\Gamma_k[\phi_a, \Psi, \bar{\Psi}]$, which is essentially the Legendre transform of a regulator-modified action

$$\mathcal{S} \mapsto \mathcal{S} + \int \frac{d^D q d^D p}{(2\pi)^{2D}} \left[\frac{1}{2} \phi_a(-q) R_{ab,k}^{(B)}(q, p) \phi_b(p) + \bar{\Psi}(q) R_k^{(F)}(q, p) \Psi(p) \right], \quad (9)$$

with the bosonic regulator $R_k^{(B)}(p, q) = \left(R_{ab,k}^{(B)} \right)(q, p)$, which for any given momenta q, p is a 3×3 matrix in the chiral Heisenberg case ($a, b = 1, 2, 3$) and a scalar in the chiral Ising case ($a, b \equiv 0$), respectively; and the fermionic regulator $R_k^{(F)}(q, p)$, which is an 8×8 matrix acting on spin and Dirac indices. Here, we have combined the frequency and momentum integration into the integration over the relativistic D -momentum $q_\mu = (\omega, \vec{q})$, with space-time dimension D . In momentum space, the regulators, introduced here integral kernels of linear operators in field space, are usually taken to be diagonal, i.e., $R_k^{(B/F)}(p, q) = R_k^{(B/F)}(q) \delta(p - q)$.

At finite scale $k > 0$, the regulator screens the IR fluctuations with $|q| \ll k$ in a mass-like fashion, ensuring that only fast modes with momentum $|q| \gtrsim k$ give significant contributions to Γ_k . The fermionic regulator $R_k^{(F)}$ is constructed in a way that the regulator modification in Eq. (9) does not spoil the chiral symmetry. Besides a sharp-cutoff regulator it is possible (and often very useful) to employ smooth cutoff functions, which allow a continuous suppression of slow modes. For $k \rightarrow 0$ the regulator has to go to zero for all momenta, such that the modifications in \mathcal{S} vanish and the effective average action approaches the full quantum effective action, $\Gamma_{k \rightarrow 0} = \Gamma$. We choose regulator functions which for $k \rightarrow \Lambda$ are of the order of the UV cutoff Λ , $R_{k \rightarrow \Lambda}^{(B)}(q) \sim \Lambda^2$, $R_{k \rightarrow \Lambda}^{(F)}(q) \sim \Lambda$. Thus, in the UV all fluctuations are suppressed and $\Gamma_{k \rightarrow \Lambda}$ becomes (up to normalization constants) the microscopic action, $\Gamma_{k \rightarrow \Lambda} \simeq \mathcal{S}$. The effective average action thus interpolates between the microscopic action in the UV and the full quantum effective action in the IR. The concept can be viewed as a specific implementation of Wilson's approach to the renormalization group: Instead of integrating out all fluctuations at once, we divide the functional integral into integrations over shells with momentum $q \in [k, k - \delta k]$ and subsequently successively integrate momentum shell by momentum shell. Γ_k is the

effective action at an intermediate step $0 \leq k \leq \Lambda$, where the fluctuations in the functional integral with momentum $q \in [k, \Lambda]$ are integrated out. The theory then is solved, once we know the evolution of Γ_k with respect to the renormalization group time $t = \ln(k/\Lambda)$ from $t = 0$ (UV) to $t \rightarrow -\infty$ (IR). The evolution equation for Γ_k has been computed by Wetterich⁴⁷ and is given by the functional identity

$$\partial_t \Gamma_k = \frac{1}{2} \text{STr} \left[\partial_t \mathbf{R}_k \left(\Gamma_k^{(2)} + \mathbf{R}_k \right)^{-1} \right], \quad (10)$$

where $\mathbf{R}_k := \begin{pmatrix} R_k^{(B)} & 0 & 0 \\ 0 & 0 & R_k^{(F)} \\ 0 & -R_k^{(F)T} & 0 \end{pmatrix}$ and $\Gamma_k^{(2)}$ denotes the second functional derivative of the effective average action with respect to the fields ϕ_a, Ψ , and $\bar{\Psi}$, i.e.,

$$\Gamma^{(2)}(p, q) \equiv \frac{\overrightarrow{\delta}}{\delta \Phi(-p)^T} \Gamma_k \frac{\overleftarrow{\delta}}{\delta \Phi(q)}, \quad (11)$$

where we have used the collective field variable $\Phi(q) = \begin{pmatrix} \phi_a(q) \\ \Psi(q) \\ \bar{\Psi}(-q)^T \end{pmatrix}$. Note that both \mathbf{R}_k and $\Gamma_k^{(2)}$ define linear operators acting on the collective field, e.g., $(\mathbf{R}_k \Phi)(p) \equiv \int \frac{d^D q}{(2\pi)^D} \mathbf{R}_k(p, q) \Phi(q)$. STr runs over all internal degrees of freedom (momentum, spin, sublattice, valley), as well as field degrees of freedom. In the fermionic sector, it takes an additional minus sign into account, $\text{STr} \begin{pmatrix} B & * & * \\ * & F_1 & * \\ * & * & F_2 \end{pmatrix} := \text{Tr } B - \text{Tr} \begin{pmatrix} F_1 & * \\ * & F_2 \end{pmatrix}$.

While the Wetterich equation (10) is an exact identity for the evolution of Γ_k , it is generically difficult to find exact solutions. It is nevertheless perfectly possible to use it to find very satisfying approximate solutions by means of suitable systematic expansion schemes. Perturbation theory constitutes one such expansion; however, for the description of phase transitions nonperturbative expansion schemes in terms of operator or vertex expansions are often superior already at relatively low order of the expansion. In particular, an expansion in terms of the derivative has been shown to be highly suitable for the study of critical phenomena in $(2+1)$ -dimensional fermion-boson systems, yielding accurate predictions for the critical exponents.^{20–22,24,26,27} In the spirit of the derivative expansion, we apply in this work the following ansatz for the effective average action:

$$\Gamma_k = \int d^D x \left[Z_{\Psi,k} \bar{\Psi} (\mathbb{1}_2 \otimes \gamma_\mu) \partial_\mu \Psi - \frac{1}{2} Z_{\phi,k} \phi_a \partial_\mu^2 \phi_a + U_k(\rho) + \bar{g}_k \phi_a \bar{\Psi} (\sigma_a \otimes \mathbb{1}_4) \Psi \right], \quad (12)$$

with the scale-dependent wave-function renormalizations $Z_{\phi,k}$, $Z_{\Psi,k}$ and the scale-dependent Yukawa-type coupling \bar{g}_k . For symmetry reasons, the scale-dependent effective bosonic potential U_k has to be a function of the

scalar product $\rho(x) \equiv \frac{1}{2}\phi_a\phi_a$ only. It is often expanded in fields as

$$U_k(\rho) = \sum_{n=1}^{\infty} \frac{\bar{\lambda}_k^{(n)}(0)}{n!} \rho^n, \quad (13)$$

with $\bar{\lambda}_k^{(1)} \equiv \bar{m}_k^2$ denoting the scalar-field mass. This type of ansatz for Γ_k is sometimes referred to as ‘‘improved local potential approximation’’ (LPA’). The UV starting values for the flow are given by the microscopic couplings in Eq. (1), i.e.,

$$\lim_{k \rightarrow \Lambda} U_k(\rho) = \bar{m}^2 \rho + 4\bar{\lambda} \rho^2, \quad \lim_{k \rightarrow \Lambda} \bar{g}_k = \bar{g}, \quad (14)$$

and

$$\lim_{k \rightarrow \Lambda} Z_{\phi,k} = \lim_{k \rightarrow \Lambda} Z_{\Psi,k} = 1. \quad (15)$$

At lower RG scales $k < \Lambda$, we absorb the wave-function renormalization factors $Z_{\phi/\Psi,k}$ into renormalized fields as

$$Z_{\phi,k}^{1/2} \phi_a \mapsto \phi_a, \quad Z_{\Psi,k}^{1/2} \Psi \mapsto \Psi, \quad Z_{\bar{\Psi},k}^{1/2} \bar{\Psi} \mapsto \bar{\Psi}, \quad (16)$$

and use the dimensionless renormalized Yukawa-type coupling $g \equiv g(k)$ and dimensionless renormalized effective potential $u(\tilde{\rho}) \equiv u(\tilde{\rho}; k)$:

$$g^2 = Z_{\phi,k}^{-1} Z_{\Psi,k}^{-2} k^{D-4} \bar{g}_k^2, \quad u(\tilde{\rho}) = k^{-D} U_k(Z_{\phi,k}^{-1} k^{D-2} \tilde{\rho}) \quad (17)$$

with $\tilde{\rho} = Z_{\phi,k} k^{2-D} \rho$. The anomalous dimensions $\eta_{\phi/\Psi} = \eta_{\phi/\Psi}(k)$ are given by

$$\eta_{\phi} = -\frac{\partial_t Z_{\phi,k}}{Z_{\phi,k}} \quad \text{and} \quad \eta_{\Psi} = -\frac{\partial_t Z_{\Psi,k}}{Z_{\Psi,k}}. \quad (18)$$

It should be worthwhile to discuss the approximations involved in our ansatz, Eq. (12). In principle, all terms of higher order in derivative or fields being invariant under the present symmetry, could be generated under RG transformations. Schematically, they have the form

$$\bar{\lambda}_k^{(m,n)} \partial^{2m} \phi^{2n}, \quad (19)$$

$$\bar{h}_k^{(m,n)} \partial^m (\bar{\Psi} M \Psi)^n, \quad \bar{g}_k^{(m,n_1,n_2)} \partial^m \phi^{n_1} (\bar{\Psi} M \Psi)^{n_2}, \quad (20)$$

with suitable matrices $M \in \mathbb{C}^{8 \times 8}$. In other words, even if we started the RG flow with pointlike coupling constants, the renormalized couplings could develop a momentum structure, i.e., we would have to deal with coupling *functions* (in Fourier space); and, furthermore, new interactions could be generated, e.g., of the four-fermion type $(\bar{\Psi} M \Psi)^2$. The mass dimensions of these additional couplings are determined by

$$[\bar{\lambda}_k^{(m,n)}] = D - 2m - (D - 2)n, \quad (21)$$

$$[\bar{h}_k^{(m,n)}] = D - m - (D - 1)n, \quad (22)$$

$$[\bar{g}_k^{(m,n_1,n_2)}] = D - m - \frac{D-2}{2} n_1 - (D-1)n_2. \quad (23)$$

In $D > 2$, all couplings neglected in our truncation of Γ_k [Eq. (12)] thus have negative mass dimension. By contrast, the scaling dimensions of the couplings already present in our ansatz read as

$$[\bar{\lambda}_k^{(n)}] = D - (D - 2)n, \quad [\bar{g}_k] = \frac{1}{2}(4 - D). \quad (24)$$

Below four space-time dimensions, $D < 4$, $\bar{\lambda}^{(2)}$ and \bar{g}_k thus have positive mass dimension, whereas they both become marginal directly in four dimensions. We thus recover^{8,13,33} that $D = 4$ constitutes an upper critical dimension of the Gross-Neveu-Yukawa-type theories, and an anticipated critical point in $D = 4 - \epsilon$ would lie in the perturbatively accessible domain for small ϵ . In this domain, however, the higher-derivative operators from Eqs. (19)–(20) (as well as $\bar{\lambda}_k^{(n \geq 3)}$) are irrelevant in the RG sense, and we would be right to neglect them in our ansatz. Our truncation of Γ_k will therefore become exact near $D = 4$: To first order in ϵ , our predictions for the critical exponents obtained by evaluating Eq. (10) with the ansatz in Eq. (12) have to coincide exactly with the known results from the $(4 - \epsilon)$ -expansion.^{8,13} We will use this fact as a cross-check to verify the validity of our computation.

In the nonperturbative regime for not so small $\epsilon \sim \mathcal{O}(1)$, however, higher (perturbatively irrelevant) interactions can be generated by the RG flow. Aside from higher-derivative terms, higher bosonic self-interactions $\propto (\phi_a^2)^n$, $n \geq 3$ may become important and might play a quantitative role for the critical behavior. Below the UV cutoff scale, the bosonic potential $U_k(\rho)$ therefore generically incorporates terms of arbitrarily high order in ρ . This is an important advantage of the functional RG approach: Contrary to conventional methods (e.g., within the context of the $(4 - \epsilon)$ -expansion), it will prove possible to include all such higher-order terms in ρ by computing the full RG evolution of the effective potential $U_k(\rho)$. Moreover, in situations where different order parameters compete, the effect of newly generated four-fermion operators has been shown to play a decisive role.²⁵ Within the present FRG scheme, they can be straightforwardly incorporated by the ‘‘dynamical bosonization’’ technique,⁴⁸ i.e., by performing a Hubbard-Stratonovich transformation at *each* RG step. However, in our present partially bosonized models, with the single order parameter $\langle \phi_0 \rangle$ or $\langle \vec{\phi} \rangle$ at hand, we assume that four-fermion interactions do not become important at lower RG scales, and leave the dynamical bosonization technique for future improvement of our results. In a next step, one can also go beyond LPA’ by successively including the higher-derivative terms of Eqs. (19)–(20) up to some fixed m . For the purely bosonic Ising universality class, various FRG studies have included terms up to 4th order in derivative, yielding predictions which agree with high-precision Monte-Carlo measurements, e.g., in terms of the correlation-length exponent ν , within an error range of $\Delta\nu/\nu \simeq 0.5\%$.⁴⁹

IV. FLOW EQUATIONS

A. Bosonic potential

The flow equation for the bosonic potential $u(\tilde{\rho})$ is readily obtained by plugging Eq. (12) into the Wetterich equation (10), and evaluating this functional identity for constant bosonic field $\rho(x) = \rho = \text{const.}$, i.e., $\phi(p) = \phi\delta(p)$ in Fourier space, and vanishing fermionic field $\Psi = \bar{\Psi} = 0$. For this field configuration the regularized scale-dependent two-point correlator $\Gamma_k^{(2)} + R_k$ is block-diagonal and easily inverted. We obtain for the chiral Ising (chiral Heisenberg) model with $S = 0$ ($S = 2$) potential Goldstone modes:

$$\begin{aligned} \partial_t u(\tilde{\rho}) &= -Du(\tilde{\rho}) + (D - 2 + \eta_\phi)\tilde{\rho}u'(\tilde{\rho}) \\ &+ 2Sv_D\ell_0^{(B),D}(u'(\tilde{\rho}); \eta_\phi) \\ &+ 2v_D\ell_0^{(B),D}(u'(\tilde{\rho}) + 2\tilde{\rho}u''(\tilde{\rho}); \eta_\phi) \\ &- 4d_\gamma N_f v_D \ell_0^{(F),D}(2\tilde{\rho}g^2; \eta_\Psi), \end{aligned} \quad (25)$$

where we have introduced the dimensionless threshold functions $\ell_0^{(B/F),D}(\omega; \eta_{\phi/\Psi})$, which involve the remaining loop integral and incorporate the dependence on the regulator function $R_k^{(B/F)}$. Their definitions are given in the Appendix. $d_\gamma = \text{Tr}(\gamma_0^2)$ is the size of the gamma matrices, and we have abbreviated $v_D = (2\pi)^{-D} \text{vol}(S^{D-1})/4 = 1/(2^{D+1}\pi^{D/2}\Gamma(D/2))$ with space-time dimension D . We have also allowed for a general ‘‘flavor’’ number N_f , counting the number of electronic spin directions, with $N_f = 2$ in the physical case.

B. Yukawa-type coupling

In order to compute the beta function for the Yukawa-type coupling g , we first rewrite Eq. (10) as

$$\partial_t \Gamma_k = \frac{1}{2} \tilde{\partial}_t \text{STr} \ln \left(\Gamma_k^{(2)} + R_k \right), \quad (26)$$

where the derivative $\tilde{\partial}_t$ is defined to act only on the *regulator's* t -dependence (and not on $\Gamma_k^{(2)}$), i.e.,

$$\begin{aligned} \tilde{\partial}_t := \int d^D x' \left[\partial_t R_k^{(B)}(x') \frac{\delta}{\delta R_k^{(B)}(x')} \right. \\ \left. + \partial_t R_k^{(F)}(x') \frac{\delta}{\delta R_k^{(F)}(x')} \right]. \end{aligned} \quad (27)$$

Let $\kappa \equiv \tilde{\rho}_{\min}$ be the value for which the effective potential $u(\tilde{\rho})$ at scale k is at its minimum, $\partial_{\tilde{\rho}} u|_{\tilde{\rho}=\kappa} = 0$. In the IR limit, κ determines the field expectation value $\langle \frac{1}{2} \phi_a \phi_a \rangle = \lim_{k \rightarrow 0} k^{D-2} \kappa$. Due to the fermionic fluctuations, which for our theory (with $2N_f d_\gamma = 16$ fermionic degrees of freedom) will turn out to dominate the flow of the effective potential, the RG fixed point corresponding to the anticipated second-order phase transition is

located in the symmetric regime, i.e., the fixed-point potential $u^*(\tilde{\rho})$ attains its minimum at the origin and κ exactly vanishes near and at the fixed point. In what follows, it therefore suffices to compute the flow equations in the symmetric regime with $\kappa = 0$.

By splitting the two-point correlator into its field-independent propagator part $\Gamma_{k,0}^{(2)} \equiv \Gamma_k^{(2)}|_{\tilde{\rho}=\Psi=\bar{\Psi}=0}$ at which the effective average action becomes minimal and the part including the (not necessarily small) fluctuations around that minimum, $\Delta\Gamma_k^{(2)} = \Gamma_k^{(2)} - \Gamma_{k,0}^{(2)}$, we can expand the logarithm and write

$$\begin{aligned} \partial_t \Gamma_k &= \frac{1}{2} \tilde{\partial}_t \text{STr} \ln \left(\Gamma_{k,0}^{(2)} + R_k \right) \\ &+ \frac{1}{2} \tilde{\partial}_t \text{STr} \sum_{n=1}^{\infty} \frac{(-1)^{n+1}}{n} \left[\left(\Gamma_{k,0}^{(2)} + R_k \right)^{-1} \Delta\Gamma_k^{(2)} \right]^n. \end{aligned} \quad (28)$$

Plugging our ansatz Eq. (12) into Eq. (28) and evaluating for non-vanishing but constant fields $\Phi(p) = \Phi\delta(p)$, $\Psi(p) = \Psi\delta(p)$, we get the beta function for the Yukawa-type coupling by comparing coefficients of the $\phi_a \bar{\Psi}(\sigma_a \otimes \mathbb{1}_4) \Psi$ terms:

$$\begin{aligned} \partial_t g^2 &= (D - 4 + \eta_\phi + 2\eta_\Psi)g^2 \\ &- 8(S - 1)v_D \ell_{11}^{(FB),D}(u'(0); \eta_\Psi, \eta_\phi) g^4. \end{aligned} \quad (29)$$

The definition of the regulator-dependent threshold function $\ell_{11}^{(FB),D}$ is again found in the Appendix. $S = 0$ in the chiral Ising model, whereas $S = 2$ in the chiral Heisenberg model.

C. Anomalous dimensions

For computing the boson (fermion) anomalous dimensions η_ϕ (η_Ψ) we again make use of the expansion Eq. (28), which we now evaluate for non-constant boson (fermion) field $\phi = \phi(p)$ [$\Psi = \Psi(p)$, $\bar{\Psi} = \bar{\Psi}(p)$] and vanishing fermion (boson) field $\bar{\Psi} = \Psi = 0$ ($\phi = 0$), and further expand in the momentum up to order $\mathcal{O}(p^2)$ [$\mathcal{O}(p)$]. The coefficient in front of the $p^2 \phi(-p)\phi(p)$ [$\bar{\Psi}(p) i\gamma_\mu p_\mu \Psi(p)$] term determines $\partial_t Z_{\phi,k}$ ($\partial_t Z_{\Psi,k}$). With the definitions in Eqs. (18) we obtain

$$\eta_\phi = \frac{16d_\gamma N_f v_D}{D} m_4^{(F),D}(\eta_\Psi) g^2 \quad (30)$$

and

$$\eta_\Psi = \frac{8(S + 1)v_D}{D} m_{12}^{(FB),D}(u'(0); \eta_\Psi, \eta_\phi) g^2, \quad (31)$$

where we have employed the threshold functions $m_{12}^{(FB),D}$ and $m_4^{(F),D}$ (see Appendix).

V. FIXED POINTS AND CRITICAL EXPONENTS

A. $(4 - \epsilon)$ -expansion

In $D = 4 - \epsilon$ space-time dimensions for small $\epsilon \ll 1$ the flow equations simplify considerably. This provides for a non-trivial and very useful cross-check of our computation in the previous section, when comparing with the known flow equations obtained from standard Wilsonian or minimal subtraction RG schemes. We expand the effective potential $u(\tilde{\rho})$ around its minimum at $\tilde{\rho} = 0$ analogously to Eq. (13) and use the dimensionless renormalized couplings $m^2 = u'(0) = Z_{\phi,k}^{-1} k^{-2} \bar{\lambda}_k^{(1)}$ and $\lambda = \frac{1}{8} u''(0) = \frac{1}{8} Z_{\phi,k}^{-2} k^{D-4} \bar{\lambda}_k^{(2)}$. We have seen in Sec. III that $D = 4$ constitutes an upper critical dimension of our theory, and we thus expect the fixed-point values of an anticipated interacting critical point to be of the order of $m^{*2}, \lambda^*, g^{*2} = \mathcal{O}(\epsilon)$. Since higher bosonic self-interactions $\sim \phi^{2n}$, $n \geq 3$, are irrelevant near the upper critical dimension [Eq. (24)], the corresponding fixed-point couplings would be of higher order, $u^{*(n \geq 3)}(0) = \mathcal{O}(\epsilon^{n-1})$. We thus may neglect them to first order in ϵ , and the same applies to higher-derivative terms [Eqs. (21)–(23)].

For calculational simplicity, it is convenient to employ the sharp-cutoff regulator R_k^{sc} , yielding the threshold functions $\ell_0^{(\text{B/F})}(\omega; \eta_{\phi/\Psi}) = -\ln(1 + \omega) + \text{const.}$, $m_{12}^{(\text{FB}),D}(\omega; \eta_{\Psi}, \eta_{\phi}) = (1 + \omega)^{-2}$, and $m_4^{(\text{F})}(\eta_{\Psi}) = 1$. A formal definition of R_k^{sc} is given in the Appendix. We have checked numerically that our predictions for the universal quantities (such as critical exponents) are regulator-independent for $D \rightarrow 4^-$. The reason is that our ansatz for Γ_k [Eq. (12)] is exact to first order in ϵ . Using the rescaled couplings

$$\lambda/(8\pi^2) \mapsto \lambda \quad \text{and} \quad g/(8\pi^2) \mapsto g \quad (32)$$

the β -functions become for $N_f = 2$

$$\partial_t m^2 = (-2 + \eta_{\phi}) m^2 - 4(S + 3) \frac{\lambda}{1 + m^2} + 8g^2, \quad (33)$$

$$\partial_t \lambda = (-\epsilon + 2\eta_{\phi}) \lambda + 4(S + 9) \frac{\lambda^2}{(1 + m^2)^2} - 2g^4, \quad (34)$$

$$\partial_t g^2 = (-\epsilon + \eta_{\phi} + 2\eta_{\Psi}) g^2 - 2(S - 1) \frac{g^4}{1 + m^2}, \quad (35)$$

with the anomalous dimensions

$$\eta_{\phi} = 4g^2, \quad \eta_{\Psi} = \frac{S + 1}{2} \frac{g^2}{1 + m^2}. \quad (36)$$

Here, we have used $d_{\gamma} = 4$ and $v_D = 1/(32\pi^2) + \mathcal{O}(\epsilon)$. We note that Eqs. (33)–(36) are exactly the one-loop results as have been found earlier within the standard Wilsonian RG approach.⁸ In the sharp-cutoff scheme this is in fact even true right up to the exact same coupling rescaling [Eqs. (17) and (32)].

For completeness, let us quote the fixed-point values together with the corresponding universal exponents which determine the critical behavior. Aside from the fully IR repulsive Gaussian fixed point (and an assumingly unphysical zero of the β -functions at $\lambda^* < 0$) we recover the well-known Wilson-Fisher fixed point at $g^{*2} = 0$ and $\lambda^* > 0$, being repulsive in the g^2 -direction, and a fermionic critical point at

$$m^{*2} = \frac{24}{(9 + S)(7 - S)} \epsilon + \mathcal{O}(\epsilon^2), \quad (37)$$

$$\lambda^* = \frac{2}{(9 + S)(7 - S)} \epsilon + \mathcal{O}(\epsilon^2), \quad (38)$$

$$g^{*2} = \frac{1}{7 - S} \epsilon + \mathcal{O}(\epsilon^2), \quad (39)$$

which is attractive both in the λ - and the g^2 -directions. We note that the fixed-point values are of order $\mathcal{O}(\epsilon)$, as anticipated. To the present order in ϵ , this confirms *a posteriori* the validity of neglecting all higher-order interactions. Close to the critical point the correlation length scales as $\xi \propto |\delta|^{-\nu}$, with the “reduced temperature” $\delta := m^2 - m^{*2}$, measuring the distance from criticality. We find

$$1/\nu = 2 - \frac{12(5 + S)}{(9 + S)(7 - S)} \epsilon + \mathcal{O}(\epsilon^2). \quad (40)$$

For the anomalous dimensions at the critical point we get

$$\eta_{\phi} = \frac{4}{7 - S} \epsilon + \mathcal{O}(\epsilon^2) \quad \text{and} \quad \eta_{\Psi} = \frac{1 + S}{2(7 - S)} \epsilon + \mathcal{O}(\epsilon^2), \quad (41)$$

with η_{ϕ} as the usual order-parameter’s anomalous dimension, determining the scaling of the order-parameter correlation function at the critical point, $\langle \phi(x) \phi(y) \rangle_{\text{conn.}} \propto 1/|x - y|^{D-2+\eta_{\phi}}$, and the fermionic anomalous dimension η_{Ψ} , determining $\langle \Psi(x) \bar{\Psi}(y) \rangle_{\text{conn.}} \propto 1/|x - y|^{D-1+\eta_{\Psi}}$ at the critical point, respectively.⁵⁴

B. Numerical evaluation for $2 < D < 4$

For general $D \in (2, 4)$ we evaluate the flow equations [Eqs. (25), (29)–(31)] numerically. A necessary condition for reliability of our results is that the regulator-dependences of our universal predictions remain small when D is no longer close to the upper critical dimension. We check this requirement by employing both the sharp-cutoff scheme as well as the linear regulator R_k^{lin} , which is also defined in the Appendix. R_k^{lin} shares with the sharp regulator R_k^{sc} the convenient property that all occurring loop integrals can be carried out analytically. For both regulators the results for these integrals are given in the Appendix.

The defining equation for the fixed-point potential $\partial_t u^*(\tilde{\rho}) = 0$ is a second-order ordinary nonlinear differential equation [see Eq. (25)]. For any given g^2 , it can be

solved numerically.²¹ For criticality alone it is, however, just as good, and technically much more convenient, to employ a Taylor expansion around the potential's minimum at $\tilde{\rho} = 0$, as in Eq. (13). For our numerical results, we truncate this expansion after the 6th order in $\tilde{\rho}$, i.e., we neglect all interactions $\sim \phi^{14}$ and higher. The order of the polynomial truncation is chosen such that an inclusion of higher-order terms changes our predictions for the critical exponents only beyond the third digit. The error introduced by truncating the effective potential is thus much smaller than the error we expect due to the truncation of Γ_k , Eq. (12). Our results for correlation-length exponent ν and anomalous dimensions η_ϕ and η_Ψ are shown in Figs. 1–3. For clarity, we have plotted only the sharp-cutoff results, since the difference to the linear-regulator exponents is hardly visible within the given resolution of these plots. Our numerical predictions in $D = 3$ are given for both regulators in Table I for the chiral Ising ($S = 0$) universality class and Table II for the chiral Heisenberg ($S = 2$) universality class, respectively. In Table II, we have also included the exponent ω , determining the leading correction to scaling, e.g., for the correlation length $\xi \propto |\delta|^{-\nu}(1 + a_\pm |\delta|^{\omega\nu} + \mathcal{O}(\delta^2))$. Since there does not seem to be any dangerously irrelevant coupling in the problem, we expect hyperscaling to hold. Our predictions for the remaining exponents α , β , γ , and δ , obtained by the usual relations,¹² are given in Table II, too.

VI. DISCUSSION

Due to the absence of an obvious small expansion parameter in the strongly-coupled system for general $D \in (2, 4)$, the truncation-induced error is hard to control. However, since the chiral Ising universality class is by now fairly well-established it provides a useful testing ground to check the reliability of our approximation. Assuming similar performances in the two universality classes, we can therewith estimate the accuracy of our predictions in the chiral Heisenberg universality class.

A. Chiral Ising universality class

Within the $1/N_f$ -expansion, the Gross-Neveu model was solved in any dimension $2 \leq D \leq 4$ up to two-loop order, with the fermion anomalous dimension being known even up to three-loop order.^{34,35} In $D = 3$ the critical exponents read as

$$1/\nu = 1 - \frac{8}{3\pi^2 N_f} + \frac{4(632+27\pi^2)}{27\pi^4 N_f^2} = 1 - \frac{0.270}{N_f} + \frac{1.366}{N_f^2}, \quad (42)$$

$$\eta_\phi = 1 - \frac{16}{3\pi^2 N_f} + \frac{4(304-27\pi^2)}{27\pi^4 N_f^2} = 1 - \frac{0.540}{N_f} + \frac{0.057}{N_f^2}, \quad (43)$$

$$\begin{aligned} \eta_\Psi &= \frac{2}{3\pi^2 N_f} + \frac{112}{27\pi^4 N_f^2} + \frac{94\pi^2 + 216\pi^2 \ln 2 - 2268\zeta(3) - 501}{162\pi^6 N_f^3} \\ &= \frac{0.068}{N_f} + \frac{0.043}{N_f^2} - \frac{0.005}{N_f^3}, \end{aligned} \quad (44)$$

TABLE I: Critical exponents in $D = 3$ for the transition into the charge-density-wave state (chiral Ising universality class, $S = 0$, with $d_\gamma N_f = 8$) from different methods. Functional RG results (this work) in LPA' approximation and by truncating $u(\tilde{\rho})$ after 6th order in $\tilde{\rho}$, both for sharp (R_k^{sc}) and linear regulator (R_k^{lin}). Previous FRG results without truncating $u(\tilde{\rho})$. $P_{i,j}(D)$ interpolates between i th-order $(2+\epsilon)$ -expansion and j th-order $(4-\epsilon)$ -expansion results, see Sec. VI.

	$1/\nu$	η_ϕ	η_Ψ
FRG [LPA', $\mathcal{O}(\tilde{\rho}^6)$, R_k^{lin}]	0.982	0.760	0.032
FRG [LPA', $\mathcal{O}(\tilde{\rho}^6)$, R_k^{sc}]	0.978	0.767	0.033
FRG [LPA', full $u(\tilde{\rho})$, R_k^{lin}] ²¹	0.982	0.756	0.032
$1/N_f$ -expansion (2nd/3rd order) ^{34,35}	0.962*	0.776	0.044
$(2+\epsilon)$ -expansion (3rd order) ²⁸	0.764	0.602	0.081
$(4-\epsilon)$ -expansion (2nd order) ^{13,33}	1.055	0.695	0.065
Polynomial interpolation $P_{2,2}$	0.995	0.753	0.034
Polynomial interpolation $P_{3,2}$	0.949	0.716	0.041
Monte-Carlo simulations ^{33†}	1.00(4)	0.754(8)	–

* [1/1] Padé approximant, Eq. (51).

† cubic-lattice model with smaller symmetry, sign problem ignored.⁵⁰

with N_f counting the number of four-component fermion species. The exponents have also been computed up to three-loop order within an expansion around the lower critical dimension.^{28–30} For $N_f = 2$ and $D = 2 + \epsilon$, one obtains:

$$1/\nu = \epsilon - \frac{1}{6}\epsilon^2 - \frac{5}{72}\epsilon^3 = \epsilon - 0.167\epsilon^2 - 0.069\epsilon^3, \quad (45)$$

$$\begin{aligned} \eta_\phi &= 2 - \frac{4}{3}\epsilon - \frac{7}{36}\epsilon^2 + \frac{7}{54}\epsilon^3 \\ &= 2 - 1.333\epsilon - 0.194\epsilon^2 + 0.130\epsilon^3, \end{aligned} \quad (46)$$

$$\eta_\Psi = \frac{7}{72}\epsilon^2 - \frac{7}{432}\epsilon^3 = 0.097\epsilon^2 - 0.016\epsilon^3. \quad (47)$$

Here, the anomalous dimensions are known even to four-loop order.^{31,32}

The corresponding partially bosonized system, the Gross-Neveu-Yukawa model, was solved to two-loop order in $D = 4 - \epsilon$ dimensions with (for $N_f = 2$)^{13,33,55}

$$1/\nu = 2 - \frac{20}{21}\epsilon + \frac{325}{44982}\epsilon^2 = 2 - 0.952\epsilon + 0.007\epsilon^2, \quad (48)$$

$$\eta_\phi = \frac{4}{7}\epsilon + \frac{109}{882}\epsilon^2 = 0.571\epsilon + 0.124\epsilon^2, \quad (49)$$

$$\eta_\Psi = \frac{1}{14}\epsilon - \frac{71}{10584}\epsilon^2 = 0.071\epsilon - 0.007\epsilon^2. \quad (50)$$

The relationship between the Gross-Neveu model in $D = 2 + \epsilon$ and the Gross-Neveu-Yukawa model in $D = 4 - \epsilon$ is similar to the one between the nonlinear sigma model and the Ginzburg-Landau-Wilson theory (linear sigma model):¹² universality suggests that the two systems in fact describe the same critical point, just from different sides of the transition. Indeed, when further expanding the $(4-\epsilon)$ -Gross-Neveu-Yukawa exponents in $1/N_f$, one finds that the coefficients are order by order the same as those one would get by expanding the $1/N_f$ -Gross-Neveu exponents at $D = 4 - \epsilon$. We also note that the same is true for the $(2+\epsilon)$ -expansion exponents, as expected.

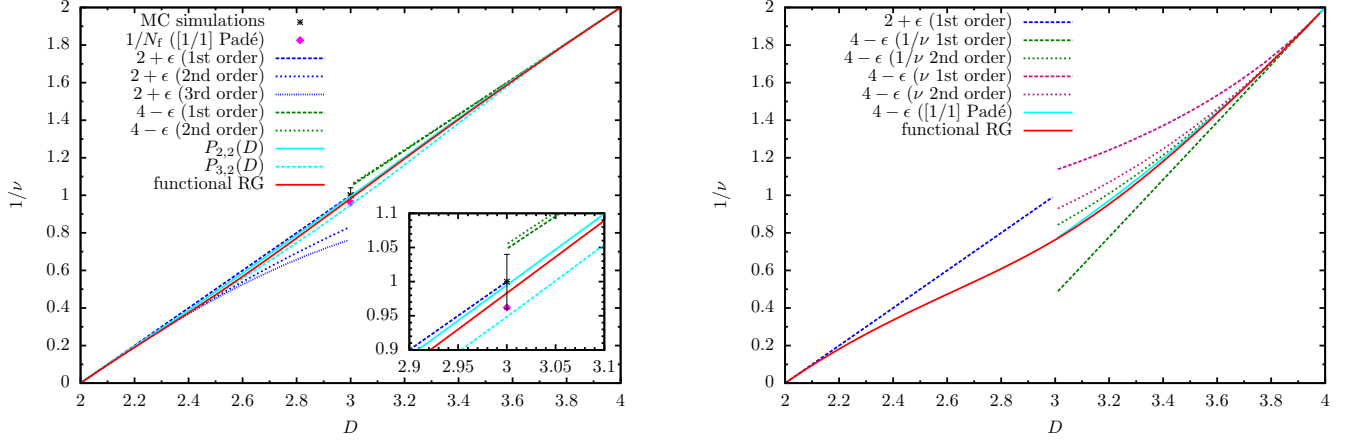


FIG. 1: Correlation-length exponent $1/\nu$ for chiral Ising (left panel) and chiral Heisenberg (right panel) universality classes from functional RG with sharp regulator (red/solid line) and for comparison from MC simulations,³³ 2nd-order $1/N_f$ -expansion ([1/1] Padé resummed),^{34,35} 3rd-order $(2+\epsilon)$ -expansion,^{28,34} 2nd-order $(4-\epsilon)$ -expansion,^{13,33} and polynomial interpolations $P_{i,j}(D)$ of i th-order $(2+\epsilon)$ - and j th-order $(4-\epsilon)$ -expansion. In the right panel we also demonstrate the ambiguity of the plain $(4-\epsilon)$ -expansion coming from either expanding $1/\nu$ or ν itself; cf. the discussion in Sec. VI.

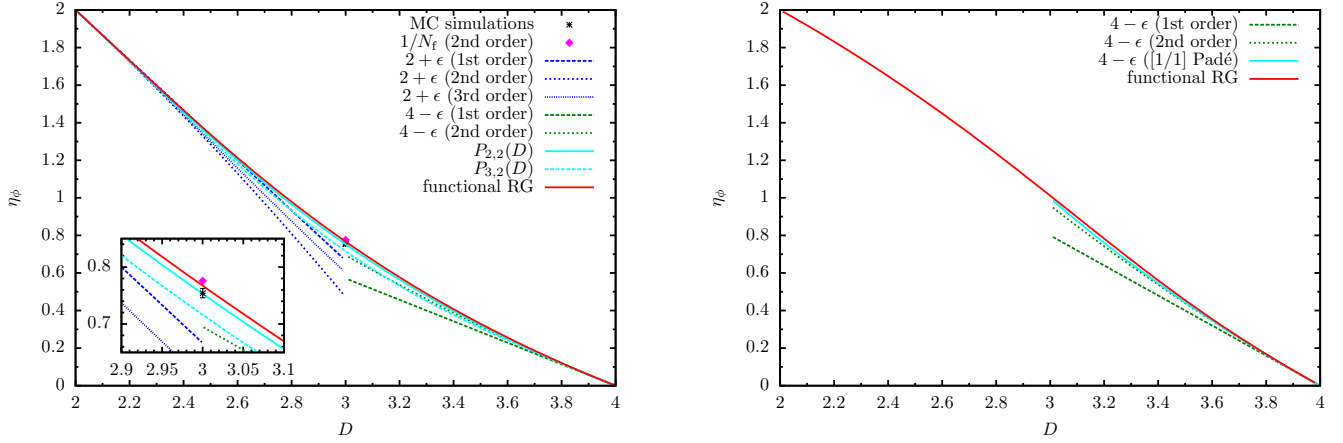


FIG. 2: Same as Fig. 1 for anomalous dimension of order parameter η_ϕ . Left panel: chiral Ising universality class. Right panel: chiral Heisenberg universality class.

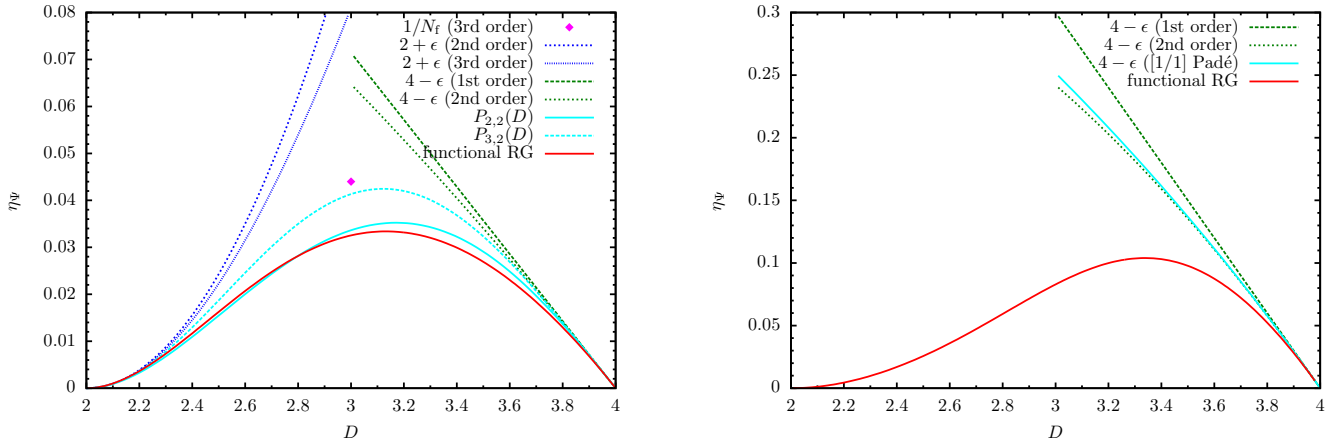


FIG. 3: Same as Fig. 1 for fermionic anomalous dimension η_ψ . Left panel: chiral Ising universality class. Right panel: chiral Heisenberg universality class.

The chiral Ising universality class has also been investigated within previous FRG calculations,^{20–22} which in some cases²¹ do not rely on an expansion of the effective potential $u(\tilde{\rho})$ as in Eq. (13), but solve the full equation for $u(\tilde{\rho})$, Eq. (25). There also exist Monte-Carlo simulations on a cubic lattice employing the staggered-fermion formulation.³³ Recent analyses⁵⁰, however, suggest that these should be taken with caution for the following reasons: Firstly, the microscopic symmetry of the cubic-lattice theory in the simulations with single species of staggered fermions (which due to fermion doubling corresponds to $N_f = 2$ four-component continuum fermions) is (besides phase rotations) $SU(2) \times \mathbb{Z}_2$ and it is not clear, whether the continuum symmetry $SU(2)_{\text{sp}} \times SU(2)_{\chi} \times \mathbb{Z}_2$ is restored close to the critical point. It is therefore not excluded that the cubic-lattice model describes a different universality class. Secondly, the standard auxiliary field approach in the staggered-fermion formulation on the cubic lattice suffers from a sign problem for $N_f = 2$, which was ignored in Ref. 33. A recently suggested approach that solves the sign problem also gives *different* critical exponents in a similar model with the same (smaller-than-continuum) symmetry group of the cubic-lattice model considered in Ref. 33.⁵⁰ The apparent consistency of the quoted cubic-lattice MC measurements with the continuum predictions (see Table I) might therefore be purely coincidental. This deserves further investigation.

ϵ - or $1/N_f$ -expansions are at best asymptotic series, and a simple extrapolation to the physical case $\epsilon = 1$ and $N_f = 2$ is quite problematic. This is particularly evident in the correlation-length exponent in the $1/N_f$ -expansion, where for $N_f = 2$ we get $1/\nu = 1 - 0.135 + 0.341 + \mathcal{O}(1/N_f^3)$, i.e., the second-order correction is in fact larger than the first-order correction, with no sign of convergence. To the present order the $(2 + \epsilon)$ - and the $(4 - \epsilon)$ -expansions are still decreasing. However, at least in parts the (superficial) convergence is rather slow, in particular for the anomalous dimensions. This is in contrast to the universality class' purely bosonic equivalent, the Ising class, where the second-order $(4 - \epsilon)$ -expansion gives exponents which agree with the best known values within an error range of less than 1%.¹² Moreover, in Eqs. (42) and (48) we have given the correlation-length exponent in each case in terms of an expansion of $1/\nu$ instead of ν itself, which is convenient in order to compare with the $(2 + \epsilon)$ -expansion, in which $\nu \propto 1/\epsilon$. A naive extrapolation to the physical case, however, leaves us with the ambiguity of either directly extrapolating the expansion of $1/\nu$ or first expanding ν itself and extrapolating $\epsilon \rightarrow 1$ afterwards. Because of the comparatively large loop corrections the difference between these two, probably equally justified, procedures is not negligible, e.g., of the order of 10% for the second-order $(4 - \epsilon)$ -expansion. All this indicates the crucial necessity of resummation of the expansions in the present fermionic systems. Standard Borel-type of resummation techniques rely on the knowledge of the large-order behavior of the coefficients,

obtained within, e.g., a semiclassical analysis.⁵¹ As far as we are aware, no such knowledge exists yet in the fermionic systems considered here.

For the correlation-length exponent in the $1/N_f$ -expansion we therefore use a naive symmetric $[1/1]$ Padé approximant⁵¹

$$[1/1]^{(1/\nu)}(N_f) = \frac{584 + 27\pi^2 + 18\pi^2 N_f}{632 + 27\pi^2 + 18\pi^2 N_f}, \quad (51)$$

where the coefficients have been chosen such that by again expanding in $1/N_f$ the Padé approximant gives back the original series in Eq. (42). Although a solid justification of the simple Padé approximation is certainly out of reach, it at least solves the ambiguity between the expansions of $1/\nu$ and ν . For the ϵ -expansions, however, one can do better: We may take advantage of the knowledge of the results from the expansions near lower and upper critical dimension *simultaneously* and try to find a suitable interpolation between these two limits. In the purely bosonic $O(N)$ models, such an interpolation algorithm, based on an optimized interpolation function within a variational approach, has been demonstrated to yield persuasively accurate values for the critical exponents⁵¹—even though the expansion around the lower critical dimension yields entirely useless values when naively extrapolating to $\epsilon = 1$. In contrast, in the fermionic systems considered here, the $(2 + \epsilon)$ - and the $(4 - \epsilon)$ -expansion yield loop corrections of comparable order, e.g., $1/\nu \simeq \mathcal{O}(1)$ in $D = 3$ while $1/\nu \rightarrow 0$ ($1/\nu \rightarrow 2$) at the lower (upper) critical dimension—a fact which makes an interpolation even more promising. To our knowledge, such a variational resummation has so far not been pursued in the case of the fermionic models. This deserves a study on its own. Here, instead of employing the full optimization process, we use a simplified approach with non-optimized interpolation function. For convenience, we employ a polynomial interpolation $P_{i,j}(D)$ between the results from the i th-order $(2 + \epsilon)$ -expansion and the j th-order $(4 - \epsilon)$ -expansion. This is done by extending the $(2 + \epsilon)$ -expansion by $j + 1$ more terms, e.g., for the correlation-length exponent ($i = 3$, $j = 2$)

$$P_{3,2}^{(1/\nu)}(D) = (D - 2) - \frac{1}{6}(D - 2)^2 - \frac{5}{72}(D - 2)^3 + a_4(D - 2)^4 + a_5(D - 2)^5 + a_6(D - 2)^6, \quad (52)$$

and fitting this extended series to the known result near the upper critical dimension, Eq. (48). I.e., we uniquely determine the coefficients a_4, a_5, a_6 by requiring

$$P_{3,2}^{(1/\nu)}(4) = 2, \quad P_{3,2}^{(1/\nu)'}(4) = -\frac{20}{21}, \quad P_{3,2}^{(1/\nu)''}(4) = \frac{325}{22491}. \quad (53)$$

By construction, the interpolating polynomial $P_{i,j}(D)$ is therefore i -loop (j -loop) exact near lower (upper) critical dimension. This interpolational resummation also solves the ambiguity between the expansions of $1/\nu$ and ν by

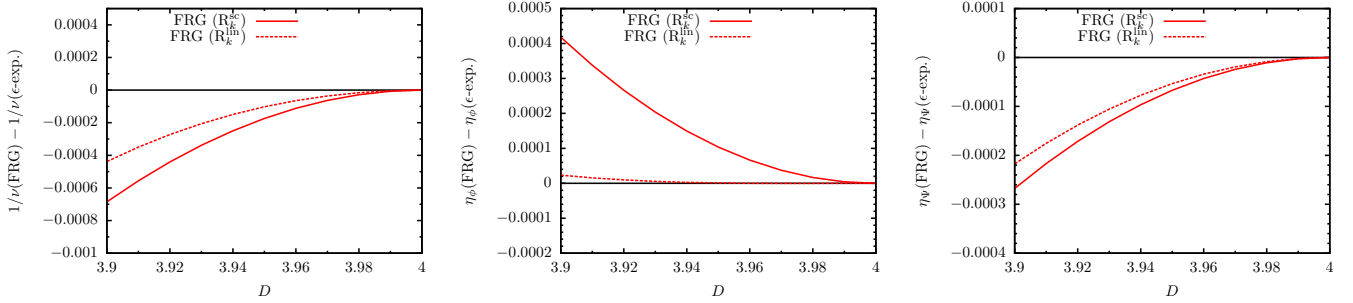


FIG. 4: Absolute difference of critical exponents from FRG with sharp and linear cutoff, respectively, to ϵ -expansion results near upper critical dimension in the chiral Ising universality class. Both sharp-cut-off and linear-cut-off scheme become numerically exact to first order in ϵ .

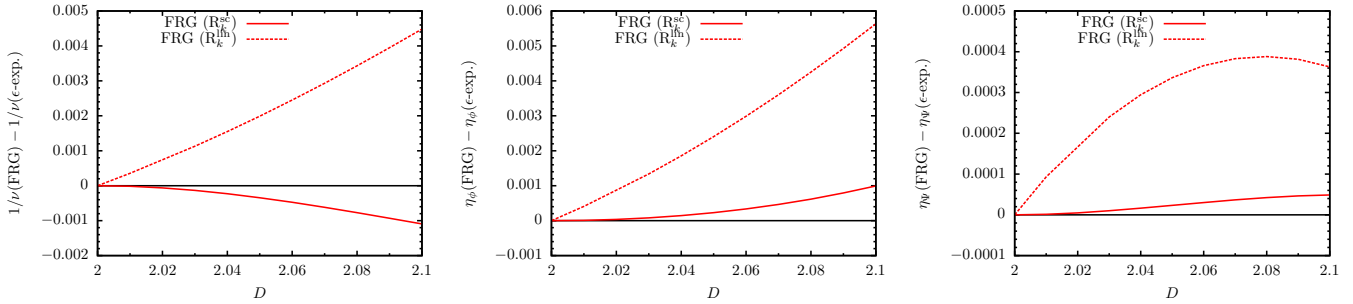


FIG. 5: Same as Fig. 4 near lower critical dimension. Here, only the sharp-cut-off scheme is numerically exact to first order in ϵ , while the linear-cut-off scheme is exact merely to zeroth order and yields slightly different first-order corrections.

construction. In order to be able to follow the development and to compare with the symmetric case $i = j$, we have computed $P_{i,j}(D)$ for both the second- ($i = 2$) and the third- ($i = 3$) order $(2 + \epsilon)$ -expansion, each with the second- ($j = 2$) order $(4 - \epsilon)$ -expansion. The results for correlation-length exponent and anomalous dimensions are shown in Figs. 1–3 (left panels), together with the naive extrapolations and our FRG predictions.

In Sec. V A it was shown that our improved local potential approximation within the sharp-cut-off scheme produces the correct one-loop exponents near the upper critical dimension, and we have checked numerically that this is also the case for the linear regulator. This is illustrated in Fig. 4, where we have plotted the absolute difference of our FRG results for both the sharp and the linear cutoff to the 2nd-order $(4 - \epsilon)$ -expansion results. Indeed, the difference as well as its derivative goes to zero as $D \rightarrow 4^-$ for both regulators. Figure 5 now shows that the sharp-cut-off FRG scheme becomes one-loop exact also near the lower critical dimension: By a linear fit to our FRG predictions in $D = 2 + \epsilon$, we in fact find for the sharp-cut-off regulator

$$1/\nu = 1.00\epsilon + \mathcal{O}(\epsilon^2), \quad (54)$$

$$\eta_\phi = 2 - 1.33\epsilon + \mathcal{O}(\epsilon^2), \quad (55)$$

$$\eta_\psi = 0.00\epsilon + \mathcal{O}(\epsilon^2), \quad (56)$$

which are on the level of our numerical accuracy ex-

actly the one-loop results from the $(2 + \epsilon)$ -expansion, cf. Eqs. (45)–(47). We note, however, that the linear regulator, which is often considered as an optimal choice,⁵² does *not* produce the exact first-order corrections near the lower critical dimension utterly: $1/\nu = 1.03\epsilon + \mathcal{O}(\epsilon^2)$, $\eta_\phi = 2 - 1.29\epsilon + \mathcal{O}(\epsilon^2)$, and $\eta_\psi = 0.01\epsilon + \mathcal{O}(\epsilon^2)$. Although small, the discrepancy to the exact coefficients from the $(2 + \epsilon)$ -expansion is numerically significant, see Fig. 5. To our knowledge, this is the first-known example in which the sharp-cut-off regulator yields substantially better predictions than the linear regulator. In light of these findings we believe that the issue of optimized RG schemes in the fermion-boson models considered here may deserve further investigation.

The numerical estimates in $D = 3$ are given for all approaches in Table I. From the size of the higher-order corrections we expect that regarding the expansions the best estimates for the anomalous dimensions η_ϕ and η_ψ are obtained from the $1/N_f$ -series, with no need for resummation. Our FRG result for η_ϕ (η_ψ) agrees with these and with the interpolation-resummed ϵ -expansion results within the mid single-digit (lower double-digit) percent range: $\Delta\eta_\phi/\eta_\phi \simeq 3 \dots 6\%$ and $\Delta\eta_\psi/\eta_\psi \simeq 20 \dots 30\%$. For the correlation-length exponent we expect either the plain two-loop $(4 - \epsilon)$ -expansion or the interpolation-resummed result to yield the most accurate value. Our FRG prediction agrees with both within $\Delta\nu/\nu \simeq 3 \dots 7\%$. Both ν and η_ϕ from the FRG

TABLE II: Critical exponents in $D = 3$ for the transition into the antiferromagnetic state (chiral Heisenberg universality class, $S = 2$, with $d_\gamma N_f = 8$) from functional RG in LPA' approximation for both linear and sharp regulator. α , β , γ , and δ from hyperscaling relations. For comparison: plain 2nd-order $(4 - \epsilon)$ -expansion results¹³ (for both the direct expansion of $1/\nu$ and the inverse of the expansion of ν , cf. text) and [1/1] Padé approximant thereof.

	$1/\nu$	η_ϕ	η_Ψ	ω	α	β	γ	δ
FRG [LPA', $\mathcal{O}(\bar{\rho}^6)$, R_k^{lin}]	0.772	1.015	0.084	0.924	-1.89	1.31	1.28	1.98
FRG [LPA', $\mathcal{O}(\bar{\rho}^6)$, R_k^{sc}]	0.761	1.012	0.083	0.908	-1.94	1.32	1.30	1.98
$(4 - \epsilon)$ -expansion ($1/\nu$ 2nd order) ¹³	0.834	0.959	0.242	—	-1.60	1.17	1.25	2.06
$(4 - \epsilon)$ -expansion (ν 2nd order) ¹³	0.923	0.959	0.242	—	-1.25	1.06	1.13	2.06
$(4 - \epsilon)$ -expansion ([1/1] Padé approx.)	0.765	0.999	0.252	—	-1.92	1.31	1.31	2.00

agree with the MC measurements within an even smaller error range: $\Delta\nu/\nu \simeq \Delta\eta_\phi/\eta_\phi \simeq 2\%$. Our findings also agree very well with the previous FRG results which solve the full equation for the effective potential, suggesting that our polynomial truncation, Eq. (13), should be just as good on our level of accuracy. We also find that our FRG predictions only slightly depend on the specific regulator function, which is additionally reassuring.

B. Chiral Heisenberg universality class

One might expect similar performances of our approximation in the chiral Ising and the chiral Heisenberg universality class. For the chiral Heisenberg universality class, there are much fewer previous calculations available; there exists, however, a two-loop calculation in $D = 4 - \epsilon$ dimensions, yielding the exponents¹³

$$1/\nu = 2 - \frac{84}{55}\epsilon + \frac{2286329}{6322250}\epsilon^2 = 2 - 1.527\epsilon + 0.362\epsilon^2, \quad (57)$$

$$\eta_\phi = \frac{4}{5}\epsilon + \frac{4819}{30250}\epsilon^2 = 0.8\epsilon + 0.159\epsilon^2, \quad (58)$$

$$\eta_\Psi = \frac{3}{10}\epsilon - \frac{6969}{121000}\epsilon^2 = 0.3\epsilon - 0.058\epsilon^2, \quad (59)$$

with again only a slow (superficial) convergence in comparison to its purely bosonic equivalent, the Heisenberg model. Again, the ambiguity between either expanding $1/\nu$ or inverting the expansion of ν itself is of the order of 10%, see Table II. At first order, it is yet considerably higher. For comparison, we have therefore also calculated [1/1] Padé approximants, analogous to Eq. (51). They are plotted together with the plain ϵ -expansion results and our sharp-cutoff FRG predictions in Figs. 1–3 (right panels). In the case of the correlation-length exponent, we compare with both the direct expansion of $1/\nu$ as well as the inverse of the expansion of ν itself, in order to demonstrate the ambiguity. The numerical estimates are given in Table II. Again, we find that our FRG approximation carries only a minor regulator dependence. ν and η_ϕ agree well with the Padé-resummed ϵ -expansions within $\lesssim 2\%$. η_ϕ agrees also with the plain second-order ϵ -expansion within $\simeq 5\%$, while ν agrees only within a somewhat larger error range $\simeq 10 \dots 20\%$, depending on whether we expand ν or $1/\nu$ in ϵ . The predictions for η_Ψ differ to about a factor of 3

between FRG and ϵ -expansion—in full analogy to the chiral Ising case, where the naive extrapolation of the $(4 - \epsilon)$ -expansion does not agree well with either FRG or the interpolational-resummation results. For completeness, we have also noted in Table II our estimate for the corrections-to-scaling exponent ω and the exponents α , β , γ , and δ , which are related to ν and η_ϕ by the hyperscaling relations.¹²

In contrast to the satisfactory agreement of our FRG predictions with those of the second-order ϵ -expansion, they appear to significantly contradict the numerical findings of the simulations of the Hubbard model on the honeycomb lattice: In Ref. 11 an excellent collapse of the finite-size-scaling data is obtained by assuming $\beta = 0.79$ and $1/\nu = 1.13$, which happen to be the values from the plain first-order $(4 - \epsilon)$ -expansion (using the extrapolation of ν itself).⁸ The exponents are $\sim 50\%$ off from our FRG predictions, and it is unlikely that a nearly as good finite-size scaling of the lattice data would be possible with our results for β and ν . Ref. 10 reports $\beta \approx 0.8$, which is close to the above quoted values, and again in clear numerical conflict with our findings. Evidently, further analytical and numerical studies would be desirable in order to pin down the values of the exponents in this universality class.

VII. CONCLUSIONS

In conclusion, we have investigated the Mott transition on the honeycomb lattice from the semimetallic phase into the charge-density wave state and into the antiferromagnetic state, respectively within an effective field-theory approach. In the Hubbard-like model, the former transition is expected for large nearest-neighbor repulsion, while the latter is induced by a strong on-site repulsion.^{5,11} They are effectively described by the chiral Ising (= \mathbb{Z}_2 -Gross-Neveu) model and the chiral Heisenberg (= $\text{SU}(2)$ -Gross-Neveu) model. We have employed the functional renormalization group formulated in terms of the Wetterich equation to compute the critical exponents, describing the critical behavior near the continuous transition. In the chiral Ising case, our predictions, made within the LPA' truncation of the derivative ex-

pansion, agree well with existing calculations up to the mid single-digit percent range for ν and η_ϕ and the lower double-digit percent range for η_Ψ . We would expect a similar accuracy in the chiral Heisenberg case, where not as many previous results exist. However, while our predictions are in agreement with the second-order $(4 - \epsilon)$ -expansion results of the chiral Heisenberg model, the significant numerical mismatch to the measurements in the Hubbard-model simulations are worrisome. These discrepancies may point to an as yet hidden subtlety in our effective Gross-Neveu-Yukawa approach, or in both our FRG approximation as well as the second-order $(4 - \epsilon)$ -expansion. This issue needs clarification in future studies. Within the FRG, a systematic improvement of the present approximation would be to incorporate the effect of newly generated four-fermion terms, e.g., by dynamical bosonization,⁴⁸ or to go beyond LPA' by including the higher-derivative terms from Eqs. (19)–(20).

Beyond its physical (and possibly technological) importance in the context of graphene, we believe that the universality classes presented in this work are an ideal testing ground to investigate the validity of nonperturbative approximation schemes, setting the stage for quantitative comparisons between field-theoretical tools. For the chiral Ising universality, we have shown that our FRG results are able to compete with the most accurate predictions from all existent other approaches. Near the upper critical dimension we have demonstrated that our predictions become universal and exact to one-loop order. This was of course to be expected, since the effective Gross-Neveu-Yukawa models considered here become perturbatively renormalizable in four space-time dimensions. In two dimensions, in contrast, these fermion-boson theories are perturbatively not directly accessible (only the purely fermionic Gross-Neveu models are) and a loop expansion directly in two dimensions should be expected to be highly scheme dependent. However, here we have demonstrated that our FRG exponents in the Gross-Neveu-Yukawa model become universal and exact also in the limit of two dimensions. Apparently, our non-perturbative LPA' truncation “knows” about the existence of the purely fermionic Gross-Neveu model with its lower critical dimension of two—in contrast to the conventional loop expansion. Near and above two dimensions, we find slight scheme dependencies. However, within the sharp-cutoff scheme, our approximation is still one-loop exact. At general dimension between lower and upper critical dimension, the FRG yields a reasonable interpolation between these two exact limits.

Acknowledgments

LJ thanks S. Chandrasekharan and H. Gies for very helpful explanations and discussions and acknowledges support by the DFG under JA 2306/1-1, GRK 1523, and FOR 723. IFH is supported by the NSERC of Canada.

Appendix: Regularized loop integrals

In this Appendix we give the details of the regularized loop integrations occurring in the derivation of our FRG flow equations. The details of the regularization scheme are encoded in the regulator functions $R_k^{(B/F)}$, which may be expressed in terms of the dimensionless shape functions $r_k^{(B/F)}$ as

$$R_k^{(B)}(q) = Z_{\phi,k} q^2 r_k^{(B)}(q^2), \quad R_k^{(F)}(q) = Z_{\Psi,k} i q r_k^{(F)}(q^2). \quad (60)$$

The Wetterich equation (10) has a one-loop structure, and the flow equations can therefore always be written in terms of one-loop Feynman diagrams. The occurring single integrals define the threshold functions; as used in this work, they are given by³⁹

$$\ell_0^{(B/F),D}(\omega; \eta_{\phi/\Psi}) = \frac{1}{2} k^{-D} \tilde{\partial}_t \int_0^\infty dx x^{D/2-1} \times \ln \left[P_k^{(B/F)}(x) + \omega k^2 \right] \quad (61)$$

$$\ell_{1,1}^{(FB),D}(\omega; \eta_\Psi, \eta_\phi) = -\frac{1}{2} k^{4-D} \tilde{\partial}_t \int_0^\infty dx x^{D/2-1} \times \left[P_k^{(F)}(x) \right]^{-1} \left[P_k^{(B)}(x) + \omega k^2 \right]^{-1} \quad (62)$$

$$m_4^{(F),D}(\eta_\Psi) = -\frac{1}{2} k^{4-D} \tilde{\partial}_t \int_0^\infty dx x^{D/2+1} \times \left[\partial_x \frac{1}{x(1+r_k^{(F)}(x))} \right]^2 \quad (63)$$

$$m_{1,2}^{(FB),D}(\omega; \eta_\Psi, \eta_\phi) = \frac{1}{2} k^{4-D} \tilde{\partial}_t \int_0^\infty dx x^{D/2} \times \frac{1}{x(1+r_k^{(F)}(x))} \partial_x \frac{1}{P_k^{(B)}(x) + \omega k^2} \quad (64)$$

where we have abbreviated the momentum-dependent parts of the inverse regularized propagator by

$$P_k^{(B)}(x) := x(1+r_k^{(B)}(x)), \quad P_k^{(F)}(x) := x(1+r_k^{(F)}(x))^2, \quad (65)$$

with $x \equiv q^2$. The scale-derivative $\tilde{\partial}_t$ acts only on the regulator's t -dependence, which implicitly occurs by means of the regularized propagator parts $P_k^{(F/B)}$. It is formally defined in Eq. (27) in the main text. The prefactors $\propto k^\alpha$ in Eqs. (61)–(64) are chosen such that the threshold functions become dimensionless.

Let us consider a one-parameter family of regulator functions, which we define in terms of their corresponding regularized inverse propagator parts

$$P_{k,a}^{(B)}(q^2) = P_{k,a}^{(F)}(q^2) = \begin{cases} ak^2 + (1-a)q^2, & \text{for } q^2 < k^2, \\ q^2, & \text{for } q^2 \geq k^2, \end{cases} \quad (66)$$

with parameter $0 < a \leq \infty$. These regulators do not affect the fast modes with $|q| > k$ at all, these modes thus give no contribution to the threshold integrals after taking the $\tilde{\partial}_t$ -derivative. Modes below but sufficiently near the RG scale k are for finite $a < \infty$ only slightly suppressed, while deep IR modes with $|q| \ll k$ are always strongly suppressed.

There are two representatives of this family of regulators, for which the threshold integrals can be carried out analytically: For $a = 1$, the regularized propagator becomes constant for slow modes with $|q| < k$, turning the integrands in Eqs. (61)–(64) into simple monomials in x . This defines the linear regulator,⁵² for which the threshold functions become²¹

$$\ell_{0; \text{lin}}^{(\text{B/F}),D}(\omega; \eta_{\phi/\Psi}) = \frac{2}{D} \left(1 - \frac{\eta_{\phi/\Psi}}{D + \frac{3\pm 1}{2}} \right) \frac{1}{1 + \omega}, \quad (67)$$

$$\ell_{1,1; \text{lin}}^{(\text{FB}),D}(\omega; \eta_{\Psi}, \eta_{\phi}) = \frac{2}{D} \left[\left(1 - \frac{\eta_{\Psi}}{D + 1} \right) \frac{1}{1 + \omega} + \left(1 - \frac{\eta_{\phi}}{D + 2} \right) \frac{1}{(1 + \omega)^2} \right], \quad (68)$$

$$m_{4; \text{lin}}^{(\text{F}),D}(\eta_{\Psi}) = \frac{3}{4} + \frac{1 - \eta_{\Psi}}{2(D - 2)}, \quad (69)$$

$$m_{1,2; \text{lin}}^{(\text{FB}),D}(\omega; \eta_{\Psi}, \eta_{\phi}) = \left(1 - \frac{\eta_{\phi}}{D + 1} \right) \frac{1}{(1 + \omega)^2}. \quad (70)$$

For large $a \gg 1$, only the modes in the thin momentum shell $[k - \delta k, k]$ with $\delta k \ll k$ give significant contributions to the threshold functions, since all lower modes are suppressed by at least $1/a$. In the sharp-cutoff limit $a \rightarrow \infty$, understood to be taken *after* the integration over the loop momentum x and the $\tilde{\partial}_t$ -derivative in Eqs. (61)–(64), the threshold functions then become²⁶

$$\ell_{0; \text{sc}}^{(\text{B/F}),D}(\omega; \eta_{\phi/\Psi}) = -\ln(1 + \omega) + \ell_0^{(\text{B/F}),D}(0; \eta_{\phi/\Psi}), \quad (71)$$

$$\ell_{1,1; \text{sc}}^{(\text{FB}),D}(\omega; \eta_{\Psi}, \eta_{\phi}) = \frac{1}{1 + \omega}, \quad (72)$$

$$m_{4; \text{sc}}^{(\text{F}),D}(\eta_{\Psi}) = 1, \quad (73)$$

$$m_{1,2; \text{sc}}^{(\text{FB}),D}(\omega; \eta_{\Psi}, \eta_{\phi}) = \frac{1}{(1 + \omega)^2}. \quad (74)$$

-
- * Electronic address: lukasj@sfu.ca
- ¹ D. C. Elias, R. V. Gorbachev, A. S. Mayorov, S. V. Morozov, A. A. Zhukov, P. Blake, L. A. Ponomarenko, I. V. Grigorieva, K. S. Novoselov, F. Guinea, and A. K. Geim, *Nature Phys.* **7**, 701 (2011).
- ² T. O. Wehling, E. Şaşıoğlu, C. Friedrich, A. I. Lichtenstein, M. I. Katsnelson, and S. Blügel, *Phys. Rev. Lett.* **106**, 236805 (2011).
- ³ M. V. Ulybyshev, P. V. Buividovich, M. I. Katsnelson, and M. I. Polikarpov, *Phys. Rev. Lett.* **111**, 056801 (2013).
- ⁴ S. Sorella and E. Tosatti, *Europhys. Lett.* **19**, 699 (1992); T. Paiva, R. T. Scalettar, W. Zheng, R. R. P. Singh, and J. Oitmaa, *Phys. Rev. B* **72**, 085123 (2005).
- ⁵ I. F. Herbut, *Phys. Rev. Lett.* **97**, 146401 (2006).
- ⁶ Z. Y. Meng, T. C. Lang, S. Wessel, F. F. Assaad, and A. Muramatsu, *Nature (London)* **464**, 847 (2010).
- ⁷ V. Juričić, I. F. Herbut, and G. W. Semenov, *Phys. Rev. B* **80**, 081405(R) (2009).
- ⁸ I. F. Herbut, V. Juričić, and O. Vafek, *Phys. Rev. B* **80**, 075432 (2009).
- ⁹ D. T. Son, *Phys. Rev. B* **75**, 235423 (2007).
- ¹⁰ S. Sorella, Y. Otsuka, and S. Yunoki, *Sci. Rep.* **2**, 992 (2012).
- ¹¹ F. F. Assaad and I. F. Herbut, *Phys. Rev. X* **3**, 031010 (2013).
- ¹² I. Herbut, *A Modern Approach to Critical Phenomena* (Cambridge University Press, Cambridge, 2007).
- ¹³ B. Rosenstein, H.-L. Yu, and A. Kovner, *Phys. Lett.* **B314**, 381 (1993).
- ¹⁴ W. Metzner, M. Salmhofer, C. Honerkamp, V. Meden, and K. Schönhammer, *Rev. Mod. Phys.* **84**, 299 (2012).
- ¹⁵ C. Platt, W. Hanke, and R. Thomale, *Adv. Phys.* **62**, 453 (2013).
- ¹⁶ C. Honerkamp, *Phys. Rev. Lett.* **100**, 146404 (2008).
- ¹⁷ M. M. Scherer, S. Uebelacker, and C. Honerkamp, *Phys. Rev. B* **85**, 235408 (2012).
- ¹⁸ M. M. Scherer, S. Uebelacker, D. D. Scherer, and C. Honerkamp, *Phys. Rev. B* **86**, 155415 (2012).
- ¹⁹ M. L. Kiesel, C. Platt, W. Hanke, D. A. Abanin, and R. Thomale, *Phys. Rev. B* **86**, 020507(R) (2012).
- ²⁰ L. Rosa, P. Vitale, and C. Wetterich, *Phys. Rev. Lett.* **86**, 958 (2001).
- ²¹ F. Hofling, C. Nowak, and C. Wetterich, *Phys. Rev. B* **66**, 205111 (2002).
- ²² J. Braun, H. Gies, and D. D. Scherer, *Phys. Rev. D* **83**, 085012 (2011).
- ²³ J. Braun, *J. Phys.* **G39**, 033001 (2012).
- ²⁴ H. Gies, L. Janssen, S. Rechenberger, and M. M. Scherer, *Phys. Rev. D* **81**, 025009 (2010).
- ²⁵ H. Gies and L. Janssen, *Phys. Rev. D* **82**, 085018 (2010).
- ²⁶ L. Janssen and H. Gies, *Phys. Rev. D* **86**, 105007 (2012).
- ²⁷ D. Mesterházy, J. Berges, and L. von Smekal, *Phys. Rev. B* **86**, 245431 (2012).
- ²⁸ J. Gracey, *Nucl. Phys.* **B341**, 403 (1990).
- ²⁹ J. Gracey, *Nucl. Phys.* **B367**, 657 (1991).
- ³⁰ C. Luperini and P. Rossi, *Ann. Phys.* **212**, 371 (1991).
- ³¹ A. Vasiliev and M. Vyazovsky, *Theor. Math. Phys.* **113**, 1277 (1997).
- ³² J. Gracey, *Nucl. Phys.* **B802**, 330 (2008).
- ³³ L. Karkkainen, R. Lacaze, P. Lacock, and B. Petersson, *Nucl. Phys.* **B415**, 781 (1994).
- ³⁴ A. Vasiliev, S. E. Derkachov, N. Kivel, and A. Stepanenko, *Theor. Math. Phys.* **94**, 127 (1993).
- ³⁵ J. Gracey, *Int. J. Mod. Phys.* **A9**, 727 (1994).
- ³⁶ J. Gonzalez, F. Guinea and M. A. H. Vozmediano, *Nucl. Phys.* **B424**, 595 (1994); *Phys. Rev. B* **59**, R2474(R) (1999); A. Giuliani, V. Mastropietro and M. Porta, *Annals Phys.* **327**, 461 (2012). I. F. Herbut and V. Mastropietro,

- Phys. Rev. B **87**, 205445 (2013).
- ³⁷ I. F. Herbut, V. Juričić, and B. Roy, Phys. Rev. B **79**, 085116 (2009).
- ³⁸ P. Kopietz, L. Bartosch, and F. Schütz, *Introduction to the Functional Renormalization Group* (Springer Verlag, Berlin, 2010).
- ³⁹ J. Berges, N. Tetradis, and C. Wetterich, Phys. Rept. **363**, 223 (2002).
- ⁴⁰ K. Aoki, Int. J. Mod. Phys., **B14**, 1249 (2000).
- ⁴¹ J. Polonyi, Central Eur. J. Phys. **1**, 1 (2003).
- ⁴² J. M. Pawłowski, Annals Phys. **322**, 2831 (2007).
- ⁴³ H. Gies, Lect. Notes Phys. **852**, 287 (2012).
- ⁴⁴ B. Delamotte, Lect. Notes Phys. **852**, 49 (2012).
- ⁴⁵ H. Sonoda, arXiv:0710.1662 [hep-th].
- ⁴⁶ A. Wipf, Lect. Notes Phys. **864**, 257 (2013).
- ⁴⁷ C. Wetterich, Phys. Lett. **B301**, 90 (1993).
- ⁴⁸ H. Gies and C. Wetterich, Phys. Rev. D **65**, 065001 (2002); S. Floerchinger and C. Wetterich, Phys. Lett. **B680**, 371 (2009).
- ⁴⁹ D. F. Litim and D. Zappala, Phys. Rev. D **83**, 085009 (2011); and references therein.
- ⁵⁰ S. Chandrasekharan and A. Li, Phys. Rev. D **88**, 021701 (2013).
- ⁵¹ H. Kleinert and V. Schulte-Frohlinde, *Critical Properties of ϕ^4 -theories* (World Scientific, Singapore, 2001).
- ⁵² D. F. Litim, Phys. Rev. D **64**, 105007 (2001).
- ⁵³ Note that for notational simplicity we use the same symbols for the fluctuating fields Ψ , $\bar{\Psi}$, ϕ_a and the arguments of Γ , i.e., the field expectation values $\langle \phi_a \rangle_{j,\eta,\bar{\eta}}$, $\langle \Psi \rangle_{j,\eta,\bar{\eta}}$, and $\langle \bar{\Psi} \rangle_{j,\eta,\bar{\eta}}$ in the presence of the conjugated sources j , η , and $\bar{\eta}$.
- ⁵⁴ Note that the factor 3 in the numerator of the Eq. (13) in Ref. 8 should be $1 + S$.
- ⁵⁵ Let us point out some typing errors in the formulas for γ_ψ and $\bar{\gamma}_{\phi^2}$ as given in Eqs. (11) and (12) of the work by Rosenstein *et al.*:¹³ In Eq. (12) in the second term of the two-loop coefficient it must read as $-94N^2$ instead of $+94N^2$ which can be seen by comparing with the formulas given by Karkkainen *et al.*;³³ additionally, only $-94N^2$ gives the correct $1/N$ expansion as quoted following Eq. (12) in Ref. 13. In Eq. (11) of Ref. 13 the one-loop coefficient misses a factor of $1/2$, as can be seen by comparing again with the expansion in $1/N$, following Eq. (11), or with Eq. (41) in the present work. Also, the two-loop coefficient as given in Eq. (11) cannot be correct, since it does not produce the correct $1/N$ expansion; we expect that in the numerator it should read $3N$ instead of $33N$, which does the job. The quoted results in the present work use these corrections.